

# Alumina/alumina composite with a porous zirconia interphase — Processing, properties and component testing

M. Holmquist<sup>a,\*</sup>, R. Lundberg<sup>a</sup>, O. Sudre<sup>b,1</sup>, A.G. Razzell<sup>c</sup>, L. Molliex<sup>d</sup>, J. Benoit<sup>d</sup>,  
J. Adlerborn<sup>e</sup>

<sup>a</sup>*Volvo Aero Corporation, 461 81 Trollhättan, Sweden*

<sup>b</sup>*ONERA, B.P. 72, 92322 Châtillon Cedex, France*

<sup>c</sup>*Rolls-Royce plc, P.O. Box 31, Derby DE24 8BJ, UK*

<sup>d</sup>*Snecma, Villaroche Centre, 77550 Moissy-Cramayel, France*

<sup>e</sup>*AC Cerama AB, Box 501, 915 23 Robertsfors, Sweden*

Accepted 18 August 1999

---

## Abstract

Novel oxide ceramic composites (NOCC) was a four year European programme aimed to develop an all-oxide ceramic matrix composite (CMC) and processing route, carry out a characterisation programme on the material and demonstrate it in a combustor rig at conditions representative of a gas turbine engine. The fibre used was a single crystal monofilament (Saphikon Inc.), which was chosen for its temperature and creep resistance. Alumina (aluminium oxide) was chosen for the fibre and matrix, and zirconia as a weak interphase coating on the fibre. Tape casting followed by hot pressing was chosen as the manufacturing route for the composite, with hot isostatic pressing (HIPping) as an alternative densification process. Cross-ply material with fibre volume fractions of around 30% was found to have moderate strength (100–130 MPa), but retained composite properties at elevated temperatures and after extended periods at elevated temperatures (1000 h at 1400°C). In addition, the material was found to withstand thermal cycling (> 1300 cycles to 1200°C), retaining its as-fabricated properties. Computational fluid dynamics (CFD) calculations were carried out for a combustor rig, and a CMC tile was designed. The temperatures, stresses and strains in the tile were predicted using finite element (FE) analysis and combustor tiles were manufactured. A tile was successfully tested in a rig at temperatures > 1260°C and up to 46 cycles. Some of the issues that remain to be addressed with the material and manufacturing method are cost, delamination during manufacture, and consistency. It is likely that, due to the high cost of the fibre and relatively modest usable strength, the material will remain as a model material. The promising results on long term static and cyclic ageing proves that the concept of an all-oxide CMC is valid and points the way to future development of this class of material. © 2000 Elsevier Science Ltd. All rights reserved.

**Keywords:** Al<sub>2</sub>O<sub>3</sub> fibre; Al<sub>2</sub>O<sub>3</sub> matrix; Composites; Gas turbine; Interphase; Mechanical properties; Thermal shock resistance

---

## 1. Introduction

Great efforts are being made among gas turbine manufacturers throughout the world to pursue technology for reducing pollutant emissions (nitrogen oxides — NO<sub>x</sub>, carbon monoxide — CO and unburned hydrocarbons — UHC) in the exhaust. Three promising methods for reducing emissions are LP (Lean Pre-mixed), LPP (Lean Pre-mixed Pre-vaporised) and RQL

(Rich burn–Quick quench–Lean burn) combustors, which lower the emissions by controlling the combustion temperature within a narrow temperature range.<sup>1</sup> These methods require the usage of hot uncooled combustor liner walls to prevent (1) incoming cooling air from locally quenching the combustion (i.e. increase UHC and CO) or (2) raising the temperature by decreasing fuel to air ratio (i.e. increase NO<sub>x</sub>). Candidate materials for this application are ceramic matrix composites (CMCs) that can withstand the temperature of the hot gas in the reaction zone, without film air cooling used in conventional combustors made from nickelbase superalloys today. With only back-cooling

---

\* Corresponding author.

<sup>1</sup> Now at: Rockwell International Corp., Science Centre, 1049 Camino Dos Rios, Thousand Oaks, CA 93106, USA.

the wall temperature of a CMC liner may be kept in the range of 1200–1400°C while ensuring a suitable uniform combustion temperature.

The envisaged application of CMC in combustor liners requires that the component resist thermal loads. These applications are designed to have minimal requirements for components to withstand pressure or other mechanical loads. In these cases, the failure strain of the composite is the most important measure of its damage tolerance. The causes of thermally induced strains include thermal mismatch with surrounding components, temperature gradients within the component and transient strains during temperature cycling.<sup>2</sup> The expected properties needed are temperature stability to 1400°C, oxidation resistance, mechanical stability, chemical stability, damage tolerance and thermal shock resistance. These properties must be maintained for long times (> 10,000 h) and under cyclic conditions.

Two classes of CMCs are considered for this application: oxide and non-oxide materials. Most development work has been done on non-oxide materials and commercial variants are usually based on silicon carbide (SiC) fibres (i.e. Nicalon<sup>TM</sup> or Tyranno<sup>TM</sup>) with a SiC or an oxide (i.e. Al<sub>2</sub>O<sub>3</sub>) matrix. They have a fibre/matrix interphase of carbon (C) or boron nitride (BN) that contain weakly bonded planes of atoms, providing a weak debond layer which imparts a non-brittle fracture behaviour. Non-oxide CMCs have attractive high temperature properties, such as creep resistance and microstructural stability. They also show high thermal conductivity and low thermal expansion, which reduces thermally induced strains. However, the oxidation sensitivity of the interphase will cause embrittlement of the composite after service at high temperatures for long times. Embrittlement is most severe with cyclic mechanical and thermal loading beyond the proportional limit, because oxygen that penetrates via the matrix cracks created will react locally with the fibres and fibre coatings to form oxide products. These reaction products will create strong bonds between the fibre and matrix, which prevent crack deflection and suppress internal frictional mechanisms that otherwise give toughness.

A way to avoid the oxidation problem is to use all-oxide composites (i.e. the composites consist of oxide fibres, oxide interfacial coatings and oxide matrices). The components are fully oxidised and further damage by oxidation can be avoided, even at high temperatures and after matrix cracking. Oxide composites also have the attractive feature of potentially low cost. The primary difficulties with this approach are the lack of suitable oxide fibre reinforcement and the lack of oxide based “debond” layer analogous to carbon or boron nitride. Most oxides also have low thermal conductivity and high thermal expansion, leading to high thermally induced strains.

Polycrystalline oxide based fibres (e.g. Nextel<sup>TM</sup> 610 or Nextel 720) have temperature limitations < 1100°C

associated with creep and sintering due to the high diffusivities of oxides compared to SiC. Single crystal oxides, particularly complex oxides (e.g. YAG), are known to have significantly better creep behaviour than polycrystals, although fabricating fibres remains a challenge. However, a single crystal alumina fibre (Saphikon<sup>TM</sup>) is commercially available having a higher temperature capability and better creep resistance than polycrystalline alumina fibres. This fibre, which is produced by the edge film fed growth method from molten alumina, has the disadvantage of being monofilament (diameter 125 µm) which prevents weaving and forming into complex shapes, and a very high cost (due to the manufacturing method). Several concepts for fibre coatings that would improve the damage tolerance of oxide CMCs have been proposed but the performance of these have only been demonstrated in model composites.<sup>3–10</sup>

## 2. Objective

The objective of the “Novel Oxide Ceramic Composites” programme was to develop an all-oxide composite for long life-time applications (> 10,000 h) at temperatures above 1400°C in oxidising environments.<sup>11</sup> Design and development of an oxide interphase has been reported previously.<sup>14–16</sup> This paper reports on the development and scale-up of a composite fabrication process, results from mechanical testing as well as fabrication and combustor rig tests of a model component.

## 3. Experimental

### 3.1. Materials

Single crystal continuous  $\alpha$ -Al<sub>2</sub>O<sub>3</sub> sapphire fibres with a nominal diameter of 125 µm (Saphikon, USA) were chosen for this project since they have a thermodynamic stability compatible with the temperature goal and forming limitations were not an issue for flat combustor tiles. However, this single crystal fibre may not be the ultimate candidate for this application due to its limited high-temperature properties<sup>12</sup> and sensitivity to slow crack growth,<sup>13</sup> but rather provide a model material on to which to base an oxide/oxide CMC. Alumina was chosen as a matrix to minimise thermally induced stresses between the fibre and the matrix and limit undesired chemical reactions. A small amount of zirconia was added to control matrix grain growth at elevated temperatures. Zirconia has been identified as a suitable interphase material in alumina based composites since the system is thermochemically stable.<sup>3</sup> However, in order for the interphase to behave as a debond layer, it is necessary to reduce the strength by introducing porosity (a porosity level of 30% has been suggested<sup>4</sup>). An

optimised zirconia coating based on a powder slurry technique was developed using a proprietary process.<sup>15,16</sup> The zirconia slurry contained a binder and carbon black powder ( $\text{ZrO}_2/\text{C}$  volume ratio was 1:1). The matrix slurry was prepared by dispersing alumina powder (SM8, Baikowski, France) and 5 vol% unstabilised zirconia powder (Degussa, Germany) in water using classical dispersion techniques.

### 3.2. Composite processing

A process based on prepreg technique was developed, Fig. 1. Single crystal alumina fibres were first passed through the zirconia slurry. After drying, the coated fibre was wound around an alumina/zirconia powder tape placed on top of a large diameter spool. An alumina/zirconia layer was tape-cast directly onto the spool and allowed to dry. Prepregs were then cut and stacked to form cross-ply green composite preforms. Composites were hot pressed in a graphite die under nitrogen atmosphere according to the temperature schedule established previously ( $1400^\circ\text{C}$ , 10 MPa, 70 min<sup>15</sup>) and finally heat-treated at  $1250^\circ\text{C}$  to remove the carbon in order to form the porous zirconia interphase. Composite plates ranging in size from  $50 \times 50 \text{ mm}^2$  to  $180 \times 200 \text{ mm}^2$  were made using this manufacturing method. Results from two full size plates (plates 4 and 5,  $180 \times 200 \text{ mm}^2$ ) are presented and discussed in this report. Interphase coating process conditions were slightly changed from plate 4 to plate 5. The purpose was to make a thinner coating (but keeping the same porosity level) in order to increase the fibre/matrix load transfer. This was achieved by decreasing the slurry viscosity. A  $[0/90]_{8,s}$  stacking sequence was used to obtain a symmetrical and balanced composite plate. Hot isostatic pressing was evaluated as an alternative to the hot pressing process. Specialised tooling was designed to keep the plates flat during processing and suitable encapsulation technique developed. Results from HIPing are reported separately.<sup>17</sup>

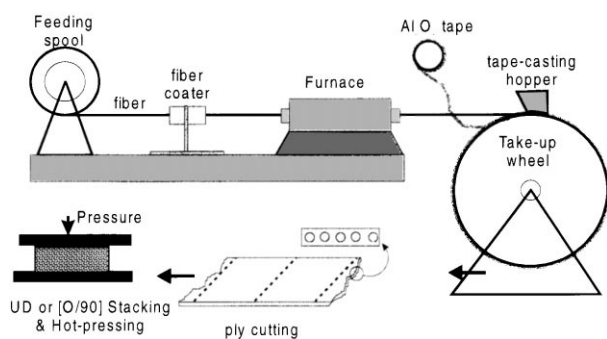


Fig. 1. Schematic illustration of fabrication process of ceramic matrix composites.

### 3.3. Evaluation

Tensile testing was done using 200 mm long test bars, gauge length 40 mm, at room temperature and elevated temperatures (800, 1200 and  $1400^\circ\text{C}$ ). An induction furnace with a susceptor was used in the high temperature testing. The test temperature was controlled by a thermocouple on the specimen in its centre. Tensile testing was also carried out on 100 mm long samples with 20 mm gauge length at room temperature in the as-received condition, after static thermal ageing for 100 and 1000 h at  $1400^\circ\text{C}$  in air and after cyclic thermal ageing tests. The cyclic thermal ageing was carried out using a 17 min cycle;  $20^\circ\text{C} \rightarrow 1200^\circ\text{C} \rightarrow 20^\circ\text{C}$ . Forced air-cooling was used and the sample experienced a severe cooling regime because it was only cooled from one side. A servo-hydraulic MTS testing system with hydraulic collet grips and a cross-head displacement rate of 0.5 mm/min was used. Strain was monitored by uniaxial or biaxial extensometers. Microstructural features of composite cross-sections and fracture surfaces were characterised using optical and scanning electron microscopy.

### 3.4. Component testing

The applicability of the composite as a material for uncooled combustor walls was assessed by evaluation in a combustor test rig operating at conditions realistic of a gas turbine combustor.<sup>1,19</sup> The rig consists of a square frame with effusion cooled nickel alloy walls which are attached with bolts. One side of the combustor has cut-outs where flat tiles can be mounted. Ceramic tiles (approximately  $90 \times 50 \times 3 \text{ mm}^3$ ) were fabricated using the process described above and tested in these cut-outs, the front (higher temperature) tile having no holes and the rear (lower temperature) having two air dilution holes (Fig. 9). In order to predict the temperature distribution in the combustor walls, a computational fluid dynamics (CFD) calculation was carried out using FLUENT code. The thermal stresses in the tiles were then calculated by finite element (FE) methods (ANSYS code) using the temperature predictions.

## 4. Results and discussion

### 4.1. Microstructure of composites

Fibre volume fractions around 30% were achieved and the plates were approximately 2.80 mm thick with densities around 87% of theoretical. Initially there were some delamination problems. A solution was found by increasing the pressure during final sintering to 15 MPa and performing a gentle heat-treatment to  $1250^\circ\text{C}$  after the plates had been cut to test bars. A cross-section is

shown in Fig. 2. The fibre spacing is relatively well controlled. Zirconia inclusions in the matrix appear to have limited the alumina grain size as they were mostly located at grain boundaries and triple grain junctions. Some porous regions with lower density could be observed between fibres in the plane of plies. In addition, the zirconia fibre coating has been deformed into “Mickey Mouse ears” on either side of the fibres and in some cases even detached from the fibre. This is a result of the hot-pressing conditions that will enhance the axial compressive deformation (which is vertical in Fig. 2). The zirconia interphase had an average thickness of 5–10  $\mu\text{m}$ . No microstructural differences were seen between plates 4 and 5.

#### 4.2. Mechanical testing

Tensile testing at room temperature of as-received samples from plates 4 and 5 showed similar UTS (ultimate tensile strength) values, although the modulus for the samples from plate 5 was higher (193 GPa instead of 152 GPa) (Fig. 3). Both sets of samples showed classical stress/strain curves with a knee at  $\sim 100$  MPa and a low modulus section to the point of failure. For plate 4, very long (up to 50 mm) pull-out lengths were observed and only a few matrix cracks appeared after the matrix cracking stress had been reached. This behaviour was thought to originate from the low load transfer to raise the stress on the composite around a main crack and eventually initiate more cracks within the matrix. The UTS, 110 MPa was approximately halved compared to similar material with unidirectional fibre lay-up.<sup>15,16</sup> This was attributed partly to a reduction in fibre volume fraction in the tensile direction to  $\sim 15\%$ . The strain to failure was 0.45% which is comparable with the currently commercially available CMCs. For samples from plate 5 slightly higher UTS were observed. The low indicated strain to failures were caused by rupture

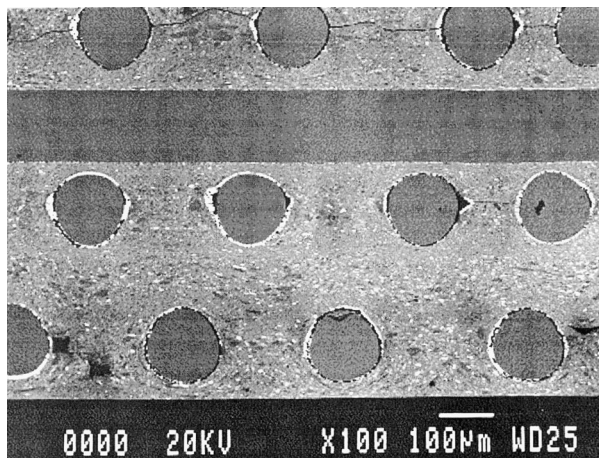


Fig. 2. Microstructure of hot pressed  $[0/90]_{8,s}$  composite.

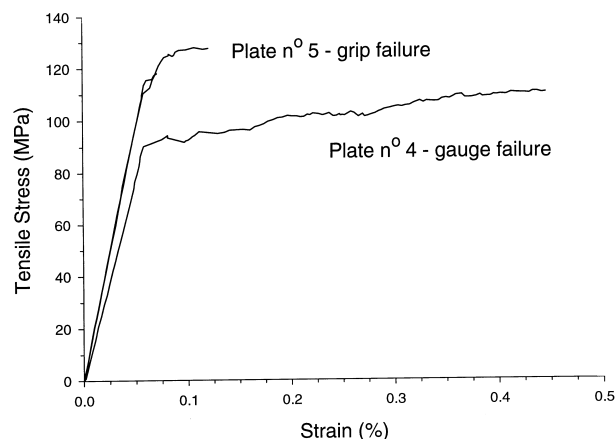


Fig. 3. Room temperature tensile stress/strain curves of as-received  $[0/90]_{8,s}$   $\text{Al}_2\text{O}_3/\text{Al}_2\text{O}_3$  composite.

outside the gauge length. Smaller pull-out lengths ( $\sim 5$  mm) were noted. This indicates a stronger fibre/matrix bonding increasing the interfacial shear stress between fibre and matrix, which also was the purpose of the changes made to the interphase process.

Remains of the porous zirconia interphase layer were visible on both the fibre and the internal surfaces of the matrix hole, Fig. 4. Round shape, loose individual zirconia grains were also observed. It has been suggested that a damage zone propagates in the porous zirconia interphase. Relative sliding between fibre and matrix will then further crush the porous structure by breaking sintered necks between the grains. Eventually the porous sintered structure is transformed into individual round powder grains that are rolled between the fibre and matrix forming small “ball-bearings” that promote sliding.<sup>15</sup> Close examination of the fibre surface revealed

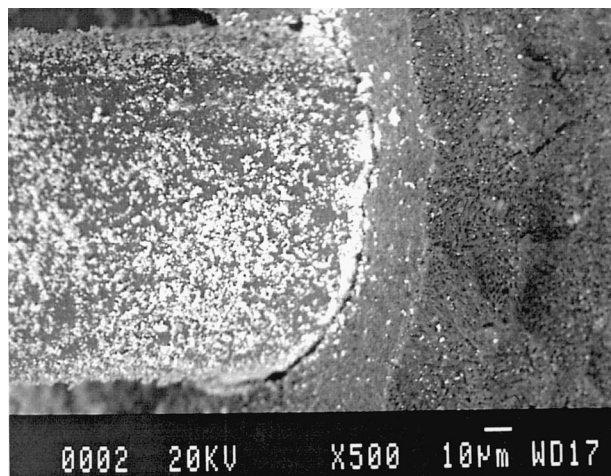


Fig. 4. Fracture surface of as-received  $[0/90]_{8,s}$   $\text{Al}_2\text{O}_3/\text{Al}_2\text{O}_3$  composite showing pulled-out fibre with remains of porous zirconia interphase layer.

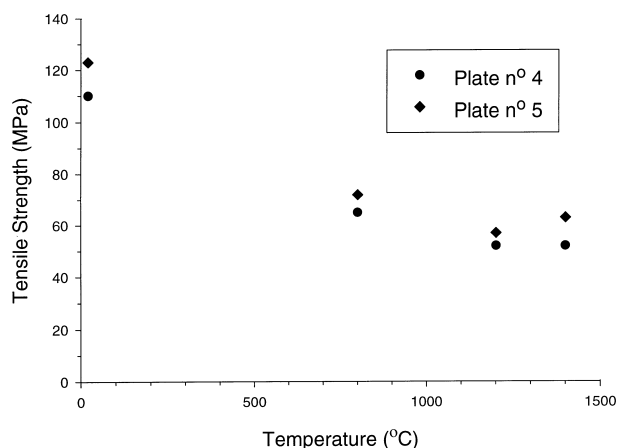


Fig. 5. UTS as a function of temperature for  $[0/90]_{8,s}$   $\text{Al}_2\text{O}_3/\text{Al}_2\text{O}_3$  composites.

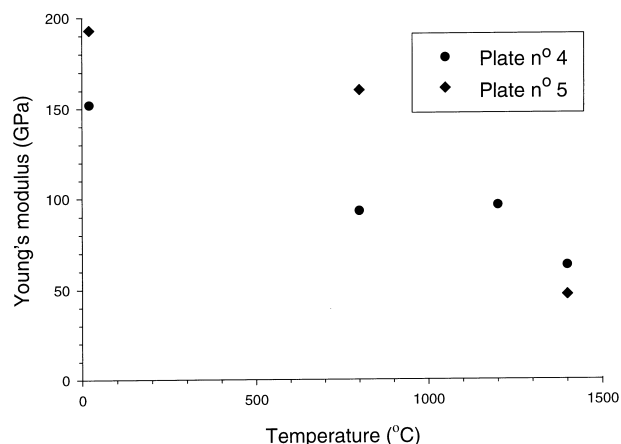


Fig. 6. Young's modulus as a function of temperature for  $[0/90]_{8,s}$   $\text{Al}_2\text{O}_3/\text{Al}_2\text{O}_3$  composites.

roughness features like sapphire surface facetting and cusps from initially sintered zirconia grains. However, these features were not thought to be too detrimental to the fibre strength.<sup>15</sup>

No significant differences between plates 4 and 5 were seen in the high temperature tensile tests (Fig. 5). At 800°C, the rate of property drop-off was 40% compared to the initial UTS. The UTS did not change between 1200 and 1400°C with 50% of room temperature (RT)

strength being retained. The modulus also dropped off as a function of temperature (Fig. 6). Examination of the fracture surfaces showed a significant reduction in fibre pull-out at 1200°C compared to RT and very little evidence of pull-out at 1400°C (Fig. 7), which is consistent with reduced fibre strength at high temperatures.<sup>20,21</sup> Scratching of the zirconia off the fibre surfaces was more evident at 1400°C, and an accumulation of zirconia was also seen on some fibres. One explanation may be that zirconia is exhibiting some plasticity at the testing temperature, modifying the “ball-bearing” mechanism.

Samples from plate 4 were aged at 1400°C for 100 and 1000 h in air and tested at RT to measure residual strength (Fig. 8). Samples aged at 1400°C, 100 h, had UTS values above 100 MPa (134 and 107 MPa) similar to the as-received sample (110 MPa) and the Young's modulus had increased slightly (to 202 and 187 GPa, respectively). No dramatic loss of properties was observed after ageing for 1000 h, one specimen even retained the initial UTS. The pull-out lengths were smaller compared to the as-received samples but still about 10 mm in length. This confirms previous bend test results<sup>15,17</sup> that composite behaviour is retained after ageing at 1400°C. However, coarsening of the zirconia interphase grains had clearly taken place during the ageing.<sup>15</sup> Grain size grew from below a micron to a few microns during the 1000-h heat-treatment. This coarsening effect could be detrimental in the long run. It has been shown that a porous structure, which is prevented from densifying, will evolve via a de-sintering mechanism<sup>18</sup> (i.e. the breaking of sintered necks leading to pore coalescence). Eventually a gap may form between fibre and matrix. The coarsening effect would, therefore, alter the load transfer mechanism but embrittlement should not occur.

One sample was subjected to thermal cycling and tested after 1367 cycles (corresponding to an accumulated time of ~230 h at 1200°C) were reached. An UTS of 148 MPa and an elastic modulus of 150 GPa was noted. The UTS is plotted in Fig. 8 for comparison with the other thermally aged samples. The results demonstrates very good thermal shock resistance for the composite material, a property that monolithic oxides otherwise do not exhibit.

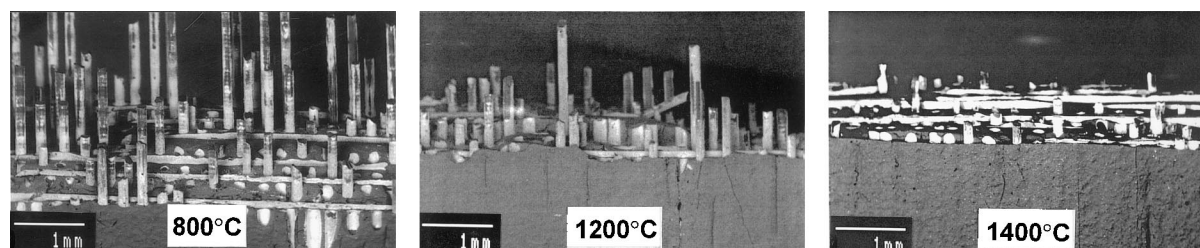


Fig. 7. Reduced fibre pull-out lengths at elevated temperatures (all samples are from plate 5).

### 4.3. Combustor rig tests

Component tiles were coated with temperature sensitive paint and tested in the combustor for 3 min. Rear tile (with air dilution holes) is shown in Fig. 10(b) (areas where the thermal paint has spalled off are white in the figure). Maximum temperatures of 1260°C were recorded. Both tiles were found to have three cracks each (8–15 mm long) running into the tile from the edges. Some microcracking (both delamination and vertical cracks) was also observed on the inside of the air dilution holes. The rear tile was then subjected to cyclic combustor rig testing for 1.5 h, corresponding to 46 cycles between idling and full load conditions. The cracks observed after the 3 min test had grown between 1 and 5 mm, and a new crack had developed on one of the edges. Some

fibre fractures were observed but the major part of the cracks was still bridged by undamaged fibres, only showing matrix damage. The expected impact of this damage on material performance is limited to matrix dominated properties such as stiffness and thermal conductivity.

Linear FE analysis was carried out of the rear tile using physical properties given in Table 1. These are a mixture of values either measured, interpolated or estimated from the literature. The linear-elastic analysis predicted a maximum stress of 239 MPa, which is higher than that measured in tensile tests of the material. Thus, it was expected that thermally induced strain would

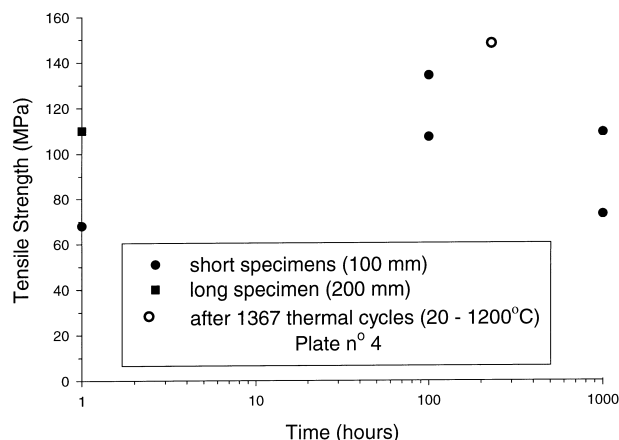


Fig. 8. Residual tensile strength at room temperature after thermal ageing at 1400°C of  $[0/90]_{8,s}$   $\text{Al}_2\text{O}_3/\text{Al}_2\text{O}_3$  composites.

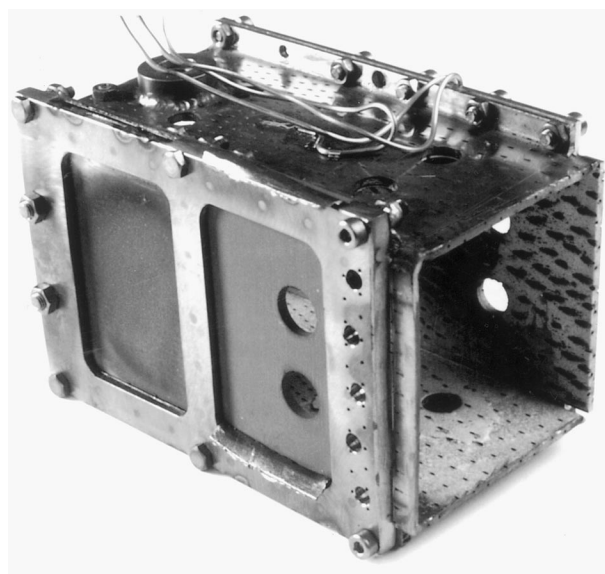


Fig. 9. Combustor can with composite tiles mounted.

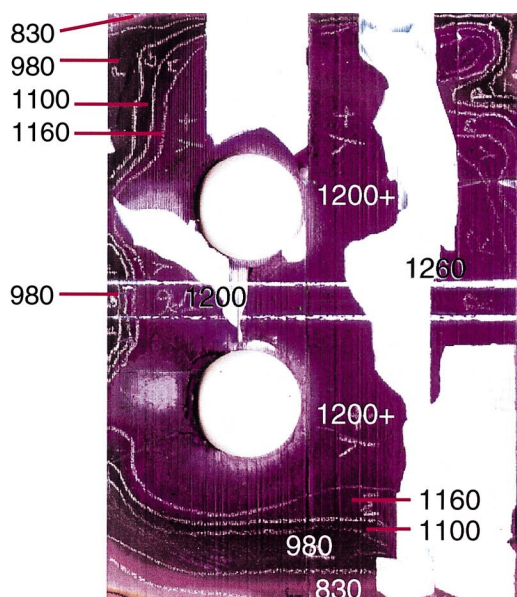
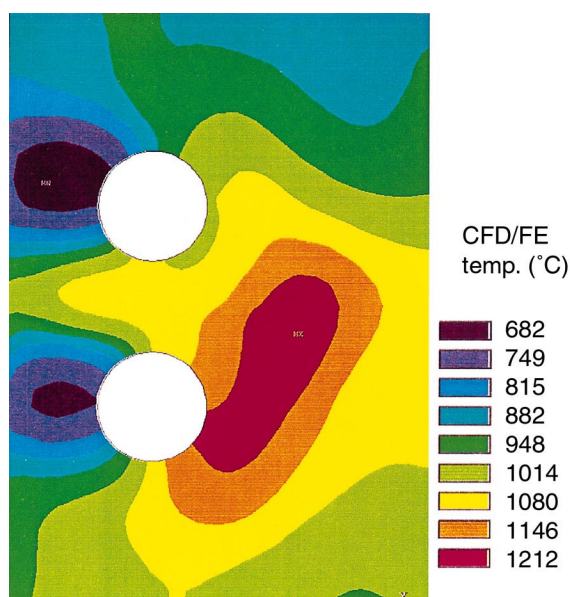


Fig. 10.  $\text{Al}_2\text{O}_3/\text{Al}_2\text{O}_3$  composite tile (hot side) showing a) calculated temperature distribution and b) temperature distribution measured in combustor rig test.



Table 1  
Physical properties used in FE analysis of  $\text{Al}_2\text{O}_3/\text{Al}_2\text{O}_3$  composite tile<sup>a</sup>

Temp (°C)	20	200	400	600	800	1000	1200	1400
$E_1$ (GPa)	155	154	151	147	141	133	115	100
$E_2$	155	154	151	147	141	133	115	100
$E_3$	110	110	107	104	101	94	82	71
$\nu_{12}\nu_{21}$	0.07	0.07	0.07	0.07	0.07	0.07	0.07	0.07
$\nu_{13}\nu_{32}$	0.10	0.10	0.10	0.10	0.10	0.10	0.10	0.10
$\nu_{31}\nu_{32}$	0.07	0.07	0.07	0.07	0.07	0.07	0.07	0.07
$\alpha_1 \times 10^{-6}$	5.30	6.70	7.50	7.85	8.10	8.30	8.50	8.70
$\alpha_2$	5.30	6.70	7.50	7.85	8.10	8.30	8.50	8.70
$\alpha_3$	5.30	6.70	7.50	7.85	8.10	8.30	8.50	8.70
$\lambda_1$ (W/mK)	13.52	7.14	5.25	4.72	4.86	4.95	5.01	5.01
$\lambda_2$	13.52	7.14	5.25	4.72	4.86	4.95	5.01	5.01
$\lambda_3$	13.13	6.93	5.10	4.58	4.72	4.81	4.86	4.86
$c_p$ (J/gK)	0.78	1.02	1.14	1.20	1.24	1.26	1.27	1.28
$\rho$ (g/cm <sup>3</sup> )	3.45							

<sup>a</sup> Fibre lay-up:  $[0/90]_{8,s}$  (i.e. 16 layers, symmetric, balanced 0.90 lay-up), assume orthotropic material properties.

result in localised matrix cracking, which should relieve stress. A non-linear (2 component linear) FE analysis was performed to allow a more accurate view of the damage accumulated by the component over a thermal cycle. The physical properties in Table 1 were used with some additions. The material was modelled as linear-elastic to the matrix cracking strain (0.059%). Upon further loading the material was supposed to follow a linear behaviour but with a substantially reduced stiffness (from 155 to 5.1 GPa). The matrix cracking strain was assumed to be temperature invariant. These assumptions were based on results from tensile testing as described previously. Due to restrictions in the ANSYS code the material properties had to be modelled

as anisotropic but temperature invariant ( $T=1000^\circ\text{C}$ ). The predictions gave a rough estimate of the temperature distribution. The temperature gradients (both through thickness and in-plane) were somewhat underestimated in the calculations, compared to the measurements (Fig. 10). The principal strain distribution is shown in Fig. 11. As can be seen, the maximum principal strain predicted for the tile is 0.329% occurring around the air dilution hole. This strain has its major component in the through thickness direction. There are also high strains along the edges (oriented parallel to the edges) of the tile. At these locations the strains are higher than the matrix cracking strain (0.059%) and localised matrix cracking is anticipated to occur as was also observed.

## 5. Conclusions

In the future, gas turbines will have to burn fuel more cleanly and efficiently for both economic and environmental reasons. In order to optimise the combustion process, minimising the generation of  $\text{NO}_x$ , CO and unburned hydrocarbons, it will be necessary to avoid film cooling of the combustor walls. Ceramic matrix composites are potential materials for these applications. All-oxide composites are inherently stable in oxidising environments at the required temperatures and offer an advantage over currently commercially available non-oxide ceramic composites.

The present investigation has shown that an alumina single crystal fibre reinforced alumina matrix is a viable concept when a porous zirconia coating allows fibre/matrix interfacial decohesion and fibre sliding upon matrix cracking. Microstructural observations of pulled-out fibres on fracture surfaces indicated that the load transfer mechanism is based on a wear effect of the porous zirconia interphase. In this process individual zirconia grains are formed which will act as ball-bearings between the fibre and the matrix. A simple in-line slurry coating technique was used to make the zirconia interphase. It was incorporated into a tape casting process to make green prepreps that were cut, stacked and hot pressed. Both unidirectional and cross-ply composite plates with dimensions up to  $180 \times 200 \text{ mm}^2$  were made in this way. Cross-ply composites had ultimate tensile strengths of 110 MPa. The strain to failure (0.45%) is comparable to other conventional CMCs with large amounts of fibre pull-out. A loss of properties with increasing temperatures was observed; at  $800^\circ\text{C}$  the strength decreased with 40% compared to the initial UTS. The UTS did not change between 1200 and  $1400^\circ\text{C}$  with 50% of RT strength being retained. The length of pulled-out fibres decreased as a function of the temperature in accordance with the decrease of the sapphire fibre strength. Composite properties were retained

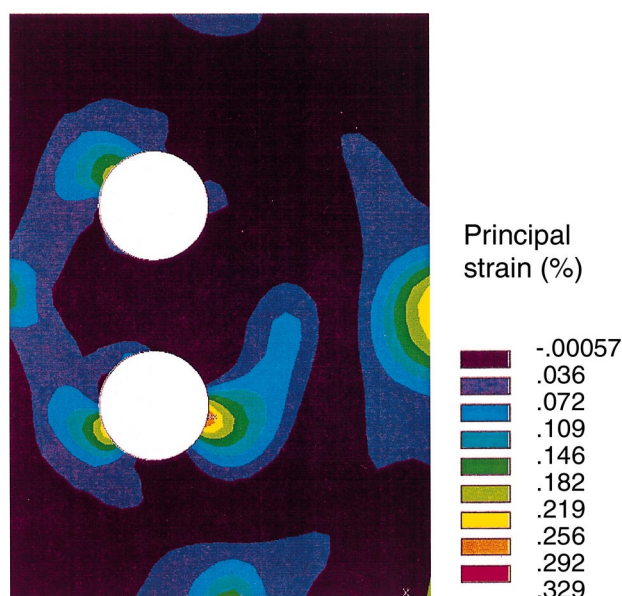


Fig. 11. Predicted strain distribution for hot side of an  $\text{Al}_2\text{O}_3/\text{Al}_2\text{O}_3$  composite tile.

even after thermal exposure of up to 1000 h at 1400°C. Although a coarsening of the porous zirconia interphase had taken place, the fracture behaviour was still non-brittle. The material also showed good resistance to thermal cycling; the as fabricated properties were retained even after > 1300 cycles to 1200°C. Flat composite tiles were fabricated and tested in a combustor rig. CFD analysis of the combustor can was used to predict gas velocities and temperatures. Material data for the composite (either predicted using constituent data from literature or measured on real material) was used in a FE model to predict material temperatures, stresses and strains. The non-linear nature of the materials stress/strain curve was approximated by using a bi-linear model. Cracking was predicted to occur locally due to thermally induced strains. After combustor testing under realistic gas turbine conditions the composite tiles exhibited limited non-catastrophic matrix cracking. Maximum temperatures of 1260°C were measured, which was very close to predicted value (1210°C).

Several issues require further work in order to make the material successful in high temperature gas turbine applications. First, a development of the fibre is needed. Most important is to improve the high temperature properties of the fibre. The cost of the fibre must also be reduced to make the material competitive on a commercial basis. A reduction in fibre diameter is required to allow more complex shapes to be manufactured. Second, the process must be developed so a higher fibre volume fraction could be achieved. There is also a need to improve the stability of the interphase. A solution might be to use an oxide interphase with slower diffusion kinetics (e.g. mullite or aluminium garnets) than zirconia to prevent sintering of the coating. It would also be beneficial to use matrix materials causing lower thermal stresses than alumina (e.g. mullite).

## Acknowledgements

Financial support from the European Commission under Brite program “Novel Oxide Ceramic Composites”, contract number BRE2-CT94-0537, is gratefully acknowledged. All the individuals within the different participating organisations, who have contributed to the success of this programme, are sincerely thanked.

## References

1. Razzell, A. G., Holmquist, M., Sudre, O. and Molliex, L., Oxide/oxide ceramic matrix composites in gas turbine combustors. ASME paper 98-GT-30, 1998.

2. Percival, M. J. L. and Beesley, C. P., Thermal strains and their effect on the life of ceramic matrix composite components in gas turbine engines. ASME paper 96-GT-533, 1996.
3. Lundberg, R., Pejryd, L., Butler, E., Ekelund, M. and Nygren, M., Development of oxide composites. In *Proceedings of High Temperature Ceramic Matrix Composites I*, ed. R. Naslain, J. Lamon and D. Doumeingts. Woodhead Publ, UK, 1993, pp. 167–174.
4. Davies, J. B., Löfvander, J. P. A., Evans, A. G., Bischoff, E. and Emiliani, M. L., Fiber coating concepts for brittle-matrix composites. *J. Am. Ceram. Soc.*, 1993, **76**(5), 1249–1257.
5. Marshall, D. B., Davis, J. B., Morgan, P. E. D. and Porter, J. R., Interface materials for damage-tolerant oxide composites. *Key Engineering Materials*, 1997, **127–131**, 27–36.
6. Faber, K. T., Ceramic composite interfaces: properties and design. *Annu. Rev. Mater. Sci.*, 1997, **27**, 499–524.
7. Morgan, P. E. D. and Marshall, D. B., Ceramic composites of monazite and alumina. *J. Am. Ceram. Soc.*, 1995, **78**(6), 1553–1563.
8. Cain, M. G., Cain, R. L., Tye, A., Rian, P., Lewis, M. H. and Gent, J., Structure and stability of synthetic interphases in CMCs. *Key Engineering Materials*, 1997, **127–131**, 37–50.
9. Lewis, M. H., Tye, A., Butler, E. and Al-Dawery, I., Development of interfaces in oxide matrix composites. *Key Engineering Materials*, 1999, **164–165**, 351–356.
10. Cinibulk, M. K. and Hay, R. S., Textured magnetoplumbite fiber-matrix interphase derived from sol-gel fiber coatings. *J. Am. Ceram. Soc.*, 1996, **79**(5), 1233–1246.
11. Novel Oxide Ceramic Composites, Brite/Euram-Project BE-7125 Contract BRE2-CT94-0537.
12. Porter, J. R., Reinforcements for ceramic-matrix composites for elevated temperature applications. *Mat. Sci. Eng.*, 1993, **A166**, 179–184.
13. Newcomb, S. A. and Tressler, R. E., Slow crack growth in sapphire fibers at 800°C to 1500°C. *J. Am. Ceram. Soc.*, 1993, **76**(10), 2505–2512.
14. Razzell, A. G., Zirconia interface layers applied to single crystal alumina fibres by PVD and CVD. *Key Engineering Materials*, 1997, **127–131**, 551–558.
15. Sudre, O., Parmentier, J., Rossignol, F., Ritti, M.-H., Vallejo, A., Sangleboeuf, J.-C. and Parlier, M., Mechanical behaviour of an alumina/alumina composite with a porous zirconia interphase. Submitted to *J. Am. Ceram. Soc.*, 1998.
16. Sudre, O., Razzell, A. G., Molliex, L., Holmquist, M. and Adlerborn, J., Alumina-single crystal fibre reinforced alumina matrix for combustor tiles. *Ceram. Eng. Sci. Proc.*, 1998, **19**(4), 273–280.
17. Holmquist, M., Lundberg, R., Eckerbom, L., Adlerborn, J., Razzell, T., Sudre, O. and Molliex, L., HIPed alumina single-crystal fibre reinforced alumina composite. Accepted for presentation at 6th ECerS, Brighton UK, 20–24 June 1999.
18. Sudre, O. and Lange, F. F., The effect of inclusions on densification: III — the de-sintering mechanism. *J. Am. Ceram. Soc.*, 1992, **75**(12), 3241–3251.
19. Holmquist, M., Lundberg, R., Razzell, A. G., Sudre, O., Molliex, L. and Adlerborn, J., Development of ultra high temperature ceramic composites for gas turbine combustors. ASME paper 97-GT-413, 1997.
20. Porter, J. R., Reinforcements for ceramic-matrix composites for elevated temperature applications. *Mat. Sci. Eng.*, 1993, **A166**, 179–184.
21. Warren, R. and Deng, S., Continuous fibre reinforced ceramic composites for very high temperatures. *Silicates Industriels*, 1996, **5–6**, 99–107.